

Influence of temperature on linear stability in buoyancy-driven fingering of reaction-diffusion fronts

D. Levitán and A. D'Onofrio

Citation: *Chaos* **22**, 037107 (2012); doi: 10.1063/1.4753924

View online: <http://dx.doi.org/10.1063/1.4753924>

View Table of Contents: <http://chaos.aip.org/resource/1/CHAOEH/v22/i3>

Published by the [American Institute of Physics](http://www.aip.org).

Related Articles

The late-time dynamics of the single-mode Rayleigh-Taylor instability

Phys. Fluids **24**, 074107 (2012)

Reduced equations of motion of the interface of dielectric liquids in vertical electric and gravitational fields

Phys. Fluids **24**, 072101 (2012)

Critical magnetic number in the magnetohydrodynamic Rayleigh-Taylor instability

J. Math. Phys. **53**, 073701 (2012)

An experimental study of small Atwood number Rayleigh-Taylor instability using the magnetic levitation of paramagnetic fluids

Phys. Fluids **24**, 052106 (2012)

Oscillatory transverse instability of interfacial waves in horizontally oscillating flows

Phys. Fluids **24**, 044104 (2012)

Additional information on Chaos

Journal Homepage: <http://chaos.aip.org/>

Journal Information: http://chaos.aip.org/about/about_the_journal

Top downloads: http://chaos.aip.org/features/most_downloaded

Information for Authors: <http://chaos.aip.org/authors>

ADVERTISEMENT



AIP Advances

Submit Now

**Explore AIP's new
open-access journal**

- **Article-level metrics
now available**
- **Join the conversation!
Rate & comment on articles**

Influence of temperature on linear stability in buoyancy-driven fingering of reaction-diffusion fronts

D. Levitán and A. D'Onofrio

Grupo de Medios Porosos, Departamento de Física, Facultad de Ingeniería, Universidad de Buenos Aires, Paseo Colón 850, (1063) Buenos Aires, Argentina

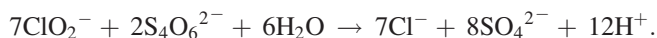
(Received 25 April 2012; accepted 4 September 2012; published online 28 September 2012)

A vertical Hele-Shaw cell was used to study the influence of temperature on Rayleigh-Taylor instabilities on reaction-diffusion fronts. The propagation of the chemical front can thus be observed, and experimental results can be obtained via image treatment. A chemical front produced by the coupling between molecular diffusion and the auto-catalysis of the chlorite-tetrathionate reaction, descends through the cell, consuming the reactants below while the product is formed above. Buoyancy-driven instabilities are formed due to the density difference between reactants and products, and the front takes a fingering pattern, whose growth rate has temperature dependence. In this study, the effect of temperature on the linear regime of the instability (that is, when the effects of such instability start to appear) was analyzed. To measure the instability, Fourier transform analysis is performed, in order to obtain the different wave numbers and their power as a function of time. Thus, the growth rate for each wave number and the most unstable wave number is obtained for each of the temperatures under study. Based on repeated experiments, a decrease in the growth rate for the most unstable wave number can be observed with the increase of temperature. © 2012 American Institute of Physics. [<http://dx.doi.org/10.1063/1.4753924>]

The aim of this work is to study the dynamic evolution of interfaces in chemical systems. These studies of instability development at reaction fronts were done experimentally in order to understand the underlying physicochemical phenomena. Fingering processes at the interface are quite common in areas as diverse as oil recovery, reservoir engineering, combustion, etc. The dynamics of the processes are complex, e.g., temperature changes and heat losses in exothermic reactions could have important effects. Due to their influence on physical and chemical processes, it is important to analyze how the fingering instability could be affected by different factors like the temperature of the medium. From the broad spectrum of fingering instabilities, we have focused on buoyancy-driven instabilities at the interface of two miscible fluids with chemical reaction. The analyzed system is a traveling front formed by an exothermic autocatalytic chemical reaction coupled to diffusion. As the denser solution is put on top of the one with smaller density, the interface remains unstable. The chemical reaction triggers a deformation at the interface modifying the fingering pattern. From the experimental point of view, the phenomena were analyzed in Hele Shaw cells. Laboratory experiments were designed and performed in order to observe instabilities produced by chemical reactions at different temperatures. Visualization techniques previously developed to observe reaction fronts and instabilities were used.

chemical front separates a solution with larger density from another one. The initially flat front which results from the coupling between the chemical kinetic and the molecular diffusion^{3,4} loses stability due to the buoyancy effects and then develops a fingering pattern.⁵

Our aim will be to analyse how the linear stability in Rayleigh-Taylor instability of reaction-diffusion front in porous media is modified by the temperature. This research is motivated by the interest of understanding and controlling the chemohydrodynamical instabilities, based on the importance of this knowledge in industry and the environmental sciences. We will use in our study the chlorite-tetrathionate (CT) acid reaction as a model system.^{6,7} The stoichiometry of the CT redox reaction becomes



When the reaction front propagates downwards, Rayleigh-Taylor type instability takes place due to the fact that the density of the upper product solution is larger than that of the reactant solution. Previous experimental and numerical works have shown that this instability can be controlled if we modify certain parameters such as: permeability of the medium where the reaction develops, external force fields (gravitational, electrical), compositions of reactants, etc.⁸⁻¹¹ The works were carried out in a Hele Shaw cell,¹² which consists of a thin layer of solution placed between two parallel flat plates with a small thickness of separation. The system behaves two-dimensionally, allowing a model of potential flow in the dynamics of fluids.²⁰ The kinetic constant of the reaction is another parameter that must be considered in these systems. This constant can be modified by controlling the temperature of the environment in which the system under study is

I. INTRODUCTION

The buoyancy-driven Rayleigh-Taylor instability takes place when a denser fluid lies on top of a lighter one in the gravitational field.^{1,2} Such a situation can be found when a

immersed. Varying the temperature of the reactor when analyzing the dynamics of an exothermic autocatalytic chemical reaction (CT reaction), could allow control over the development of the instabilities produced by the density difference. In the work done by Casado *et al.*, the effect of the temperature on these systems for the non linear regime was shown.¹³

There are a great number of theoretical works dealing with hydrodynamics of reacting interfaces,^{11,14–30} there is a need for experimental studies to provide data comparable with those of the simulation. In our study, we analyse the instability development for short times (linear systems) by measuring the most unstable wave number at different temperatures (8.4 °C to 34.9 °C) for the acid CT reaction. The most unstable wave number is defined as the wave number for which the growth rate σ_k is maximum. In previous works, it has been shown that the most unstable wave number depends not only on the difference of density between products and reactants but also on the velocity and thickness of the chemical front.^{18–20,31}

The chlorite oxidation of tetrathionate is an acid-catalyzed reaction (product) in a slight excess of chlorite. This chemical reaction is exothermic with an enthalpy of reaction $\Delta H = (-3960 \pm 50)$ kJ/mol.¹⁵ The density of the product solution (ρ_2) is larger than the density of the reactant solution (ρ_1); hence the downward travelling front is buoyantly unstable and density fingers develop over time.

We introduce the Damköhler number (Da) as the ratio between the characteristic hydrodynamic time and the characteristic chemistry reaction time. This is expressed as: $Da = \tau_h/\tau_c$. We introduce U as the characteristic speed term that appears from the viscosity and buoyant force balance as $U = (\Delta\rho gK)/\nu$, where $\Delta\rho = (\rho_2 - \rho_1)/\rho_0$ ratio between the density differences relative to that of pure water and $\nu = \mu/\rho_0$ is the kinematic viscosity. We define the hydrodynamic time scale as: $\tau_h = D_x/U^2$ and characteristic chemical time as: $\tau_c = 1/q\alpha_0^3$, where D_x is the diffusion coefficient of species, α_0 is the initial concentration of tetrathionate ion ($\alpha_0 = [S_4O_6^{2-}]_0$) and q is the reaction rate constant. With these expressions we arrive to $Da = D_x\nu^2q\alpha_0^3/(\Delta\rho gK)^2$, using $K = a^2/12$ (a is the Hele Shaw cell gap), the Da is equal to $144D_x\nu^2q\alpha_0^3/(\Delta\rho ga^2)^2$. Unfortunately, there is an uncertainty on the kinetic constant values of q and the diffusion coefficient D_x as mentioned in Ref. 13, therefore there is an uncertainty in the Da , limiting its use, but we can do a qualitative analysis of its dependence with the temperature by means of the parameters ρ , ν , and q .

The outlines of the article are the following: in Sec. II, we give a description of the system used in our experiments. The experimental results for different temperatures are shown in Sec. III. In this section, we show the dispersion relation for a particular case of temperature, the most important wave number and the maximum growth rate as functions of temperature, which are directly related to the kinetic constant of the reaction. In Sec. IV, we discuss the obtained results and conclusions are shown in Sec. V.

II. EXPERIMENTAL SETUP

We built a device consisting of a Hele-Shaw cell made of two Plexiglas plates of 20 cm \times 20 cm \times 1 cm each (Fig. 1).

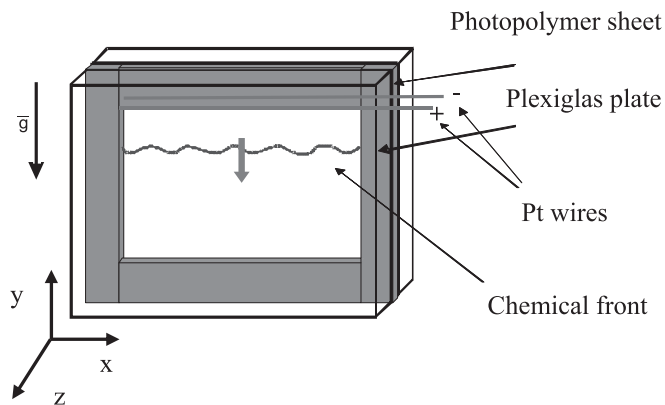


FIG. 1. Schematic representation of the Hele Shaw cell. The Pt wires that trigger the reaction are illustrated.

The cell is placed into a thermal bath at a constant temperature. We employed a Cole Parmer refrigerator model Polystat, and the temperature was measured with a Fluke II K-52 thermometer and a type-K thermocouple located inside the thermal bath.

The system is vertically oriented, with the gravity field along the y axis (Fig. 1). The initial solutions were prepared using analytical grade chemicals of the highest purity (Sigma, Aldrich, Reanal) and ultra pure water (Alpha Q). Bromophenol Blue was used as a pH indicator, which imparts a blue color to the alkaline solution (reactants) and a yellow color to the acid solution (product). The composition of the reactant solution is $[NaClO_2] = 0.020$ M, $[K_2S_4O_6] = 0.005$ M, $[NaOH] = 0.001$ M and $[Bromophenol\ Blue] = 0.1$ g/100 cm³. The cell is filled with a syringe containing the reactant solution after being cooled down to the selected temperature.

A downward planar front is induced by means of Pt-wire electrodes (0.25 mm diameter) that trigger the chemical reaction in the upper side of the cell by applying a 4 V potential difference for 4–5 s. The density of the products is larger than the one of the reactants. For density measurement, we used a densimeter (Antón Paar DMA 35N), and we measured temperature with the same densimeter. The measurement was made by placing a beaker with the solutions in a thermal bath.

The experiments were filmed and recorded using a digital video camera. The image resolution obtained was of 720 \times 480 pixels and was digitalized at 0.25 s intervals by applying programs based on language C in order to obtain the travelling front (interface position), the pattern wavelength as a function of time and the power spectral density, for each wave number. To determine the pattern wavelength, the program finds the front shape on every image and computes the power spectral densities as a function of time for the different experimental cases. Previously, we choose the image with the best contrast between reactants and product in the red-green-blue (RGB) split.

III. EXPERIMENTAL RESULTS

A vertically oriented system was tested at different temperatures in order to obtain the growth rate as a function of wave number at each temperature. The bottom part of the

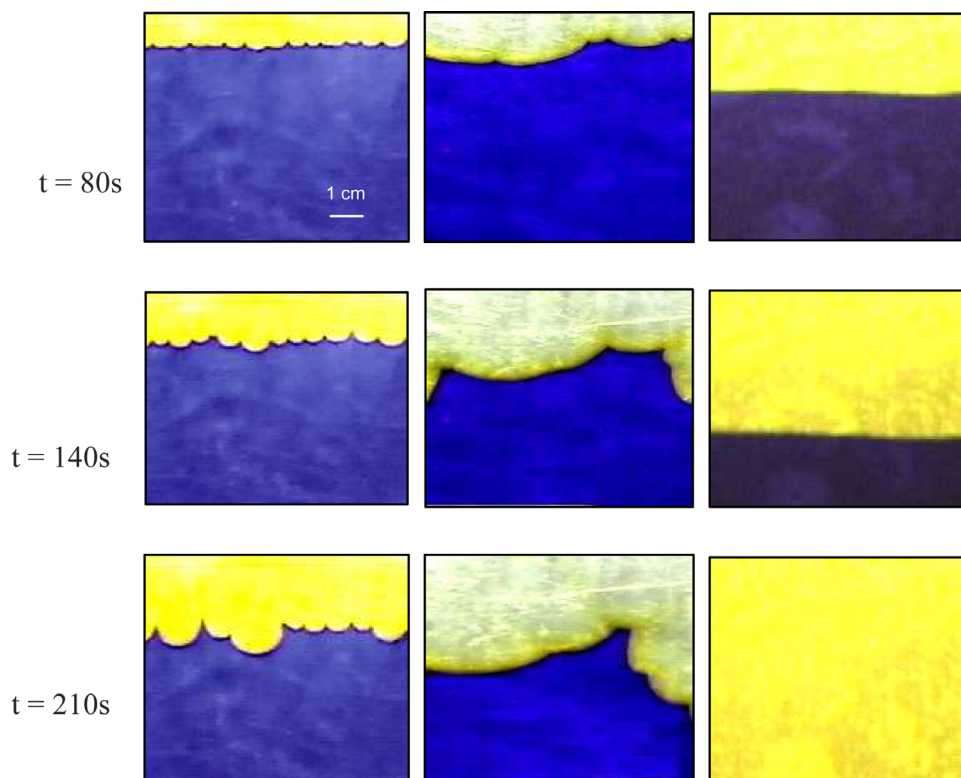


FIG. 2. Images obtained at different times: (a) $T = 12.4^\circ\text{C}$; (b) $T = 18.2^\circ\text{C}$ and (c) $T = 34.9^\circ\text{C}$. Fresh reactants are represented in the blue zone, while the product (downward orientation) is represented in the yellow zone. We can observe the waves in the chemical front and the influence of the temperature. The experiments are similar to those studied in the nonlinear regime of the dynamics in Ref. 13.

cell is filled by means of a syringe containing the reactants. The cell then remains filled with the reactants a couple of minutes in order to ensure that the whole system has the same temperature.

The chemical reaction is initiated at the top of the cell yielding a moving front. The density of the product solution is larger than that of the reactant solution; hence the travelling front is buoyantly unstable. The buoyantly instable front is modified when the chemical front velocity increases (more stable) (Fig. 2).

From the study of the length of the mixing zone (non linear system), we have found (in a previous work¹³) that this zone increases when the temperature of the system decreases. In this work, we analyze the growth rate (linear system) dependences with the temperature.

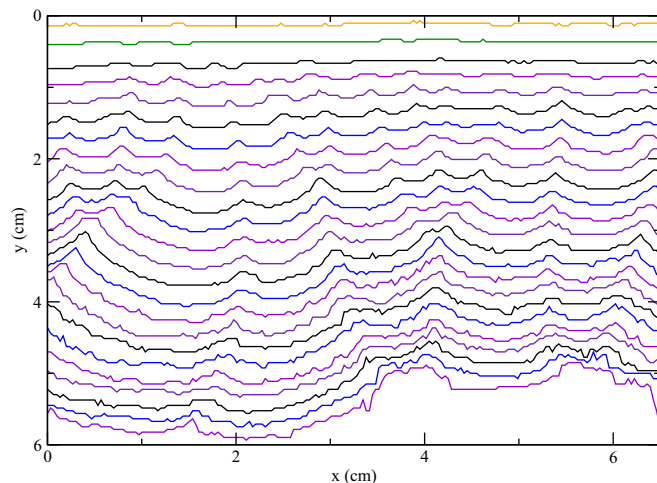


FIG. 3. Front profiles for different times for $T = 18.2^\circ\text{C}$ and $\Delta t = 3.6\text{s}$. These front profiles correspond to Fig. 2(b).

The profiles of the interface obtained after the treatment of the images (see Ref. 13) are shown in Fig. 3. We do a one-dimensional Fourier transform of the interface, and then we obtain the power spectral densities as a function of the wave number for each studied temperature (Fig. 4). Repeating this at successive times eventually gives the time dependence of the power of the most unstable mode (Fig. 5) and the slope in the linear regime gives the growth rate. The time when the system stops acting in a linear regime, and the growth rate for that time can be obtained from this type of graph. Fig. 6 shows the growth rate for different wave numbers (dispersion curve) for temperature equal to 8.5°C and 18.2°C , as an example. These results were fitted with a

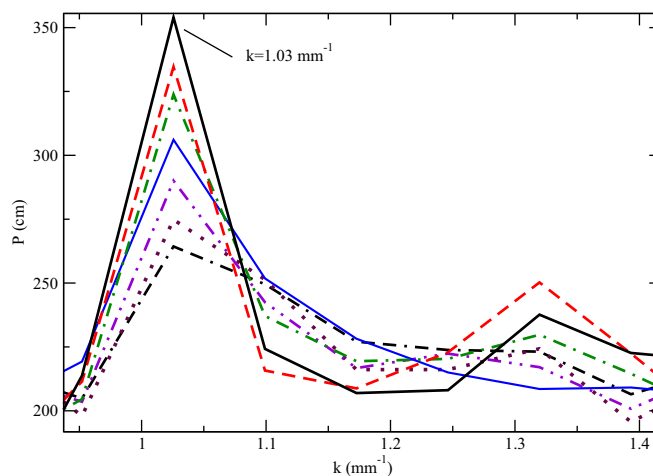


FIG. 4. Power spectral densities P of the fingers for different times. The first one is the black dotted line at 2 s and the latest one is the full black line at 14 s. Note that the basic modes ($k = 1.03\text{ mm}^{-1}$) has the maximum growth rate. The temperature is 18.2°C and Δt is 2 s.

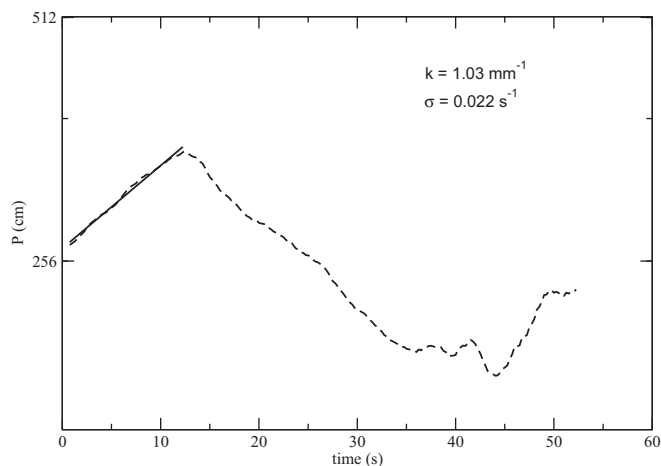


FIG. 5. The power spectral density P of the wave number k_{\max} with maximum growth rate as a function of time. The solid lines are the linear fitting for obtain the growth rate corresponding to the wave number. We can see that for large times ($t > 10$ s) the system is non-linear and the growth rate decreases. The temperature is 18.2°C .

quadratic function just to guide the eye. Although these fittings were done just to guide the eye and they do not have any physical meaning, they help to identify trends varying the temperature. The most unstable wave number k_{\max} (with maximum growth rate σ_k) can be observed. In order to calculate the growth rate, data from several experiments under the same conditions are averaged (Figs. 7 and 8). In Fig. 7, the most unstable wave number is shown for each temperature. It can be seen that there is no clear tendency with the variation of temperature, with values oscillating between 8.5°C and 25°C .

In Fig. 8, we see how the maximum growth rate σ_k decreases in a temperature range that goes from 8.5°C up to 25°C . It is also noticed that the front velocity is larger when the temperature of the system increases. This kind of phenomenon was observed in a previous experiment.¹³ Experiments were carried out at 34.9°C but at that temperature there is no instabilities, therefore it is not possible to measure the wave number and the growth rate.

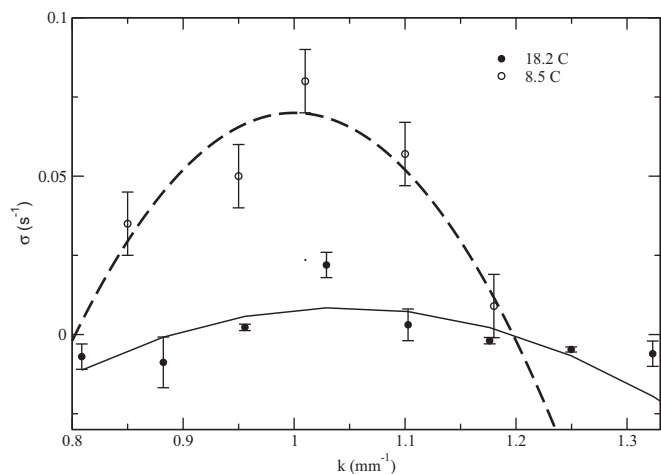


FIG. 6. Growth rate as a function of wave numbers. We can see the maximum growth rate for $k_{\max} = 1.03 \text{ mm}^{-1}$ when the temperature is equal to 18.2°C and $k_{\max} = 1.01 \text{ mm}^{-1}$ for 8.5°C . The lines are just to guide the eye.

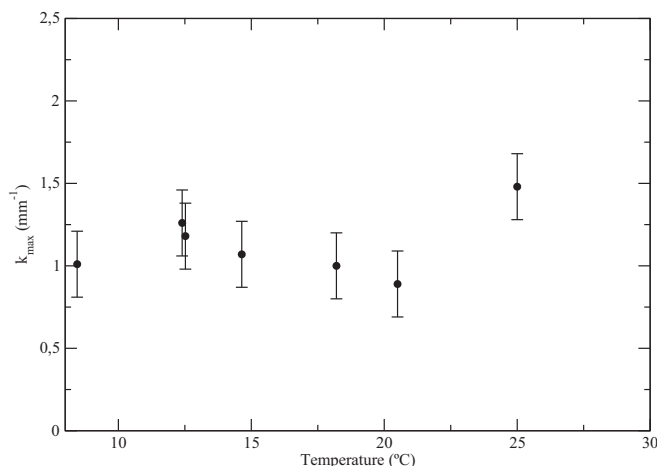


FIG. 7. Most unstable wave number as a function of temperature.

Considering Fig. 8, we can say that if temperature is increased in such a way that the kinetic constant q of the chemical reaction is the predominant factor in the number of Da , the fingers will disappear in order to achieve a stable front. We foresee this for a temperature of 39.4°C , although this situation could be also revealed at a bit lower temperature. The variation of the growth rate with temperature (Fig. 8) shows that for low temperatures the growth rate increases, while for high temperatures the value is practically close to zero.

IV. ANALYSIS AND DISCUSSION

The dependence of the Da on temperature is caused mainly by the effect of temperature on ρ , ν and q . Of these three, the most important effect is on q , the chemical reaction rate constant; as is mentioned in Ref. 13. For higher temperatures, the chemical reaction rate constant increases, then the Da increases, this means that the characteristic chemical time becomes shorter than the hydrodynamic characteristic time.

We see that as the temperature (or Da) increases, the growth rate decreases. This can be due to the strong influence of temperature on q for the reaction, which increases

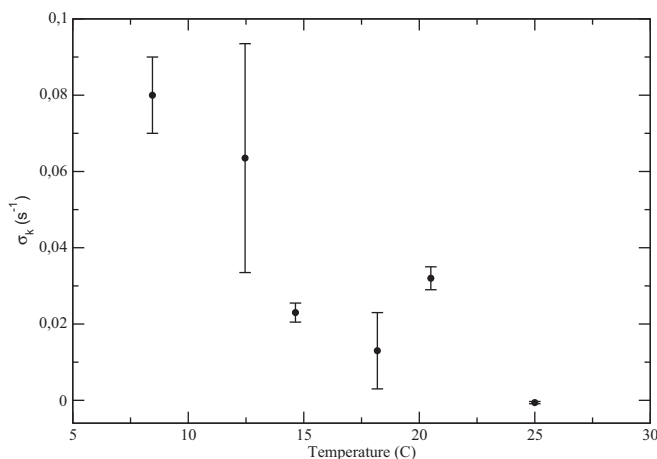


FIG. 8. Maximum growth rate σ_k for different temperatures values. Each point is the mean on several experiments.

exponentially with the increase of temperature. Thus, we find that the finger patterns formed due to buoyancy, in times close to zero are frozen in time, that is, with growth rates that are nearly zero, as can be seen for temperature 25 °C with growth rate equal to 0.0024 s^{-1} . This concurs with previous works¹³ where the mixing zone, defined as the distance between the average of the most advanced and the least advanced points for the instability, remains nearly constant for temperatures near to 40 °C. For temperatures above 39.4 °C, no linear instability analysis was performed due to the fact that no fingering patterns appear for such temperatures. Hence, since for high temperatures, the reaction velocity is much larger than the speed in which the fingers are propagated, if there are chemical reaction present at high temperatures in the system, a completely flat descending front would be observed.

In lower temperature (lower Da), we see that when the temperature decreases, a larger growth rate is observed. This is due to the fact that the speed of the front (refers to the speed at which the front moves because of coupling of reaction and diffusion) is lower, which allows the buoyancy-driven instabilities to develop, as was previously mentioned. It is necessary to emphasize that the temperature range for this work is in the range of 10–40 °C, the variation of the density gradient for water with temperature is similar but larger than the region of temperatures where it is smallest (around 4 °C). On the other hand, the exothermic CT reaction produces a local temperature variation of about 1–2 °C in the region close to the reaction front, so there is a small decrease in density in that area, producing a destabilizing effect on the front which is superimposed on the destabilizing effect of the reaction itself. In any case, both effects are stabilized when the kinetic constant increases, due to the fact that the chemical front moves faster than the buoyancy induced fingering.

No significant variation was found for the wave number with maximum growth rate with the variation of temperature. Thus, we can say that there is no effect on this from the increase of the reaction rate. This could be due to the fact that the instabilities always begin in the same conditions (the concentration of the reactants, the gap width of the Hele-Shaw cell, which is related to the permeability of the medium) except the changes of temperature. So the initial conditions for the instability were always the same, generating a similar initial wave number.

V. CONCLUSIONS

As a conclusion we can say that Rayleigh-Taylor instabilities due to self-catalyzing chemical reactions are strongly influenced by the external temperature of the system. The growth rate will be diminished if the temperature increases, producing a smaller development on the instability with

time. A different effect occurs for the wave number, which will produce a deformation of the planar wave front independent of the temperature of the reaction. Thus, controlling the temperature, the growth of the instability can be controlled, but not the front deformation.

ACKNOWLEDGMENTS

The authors wish to thank to CONICET (Argentina), FNRS (Belgium), and Universidad de Buenos Aires for their financial support.

- ¹S. Chandrasekhar, *Hydrodynamic and Hydromagnetic Stability* (Clarendon, Oxford, 1961).
- ²O. Manickam and G. M. Homsy, *J. Fluid Mech.* **288**, 75 (1995).
- ³J. D. Murray, *Mathematical Biology* (Springer, Berlin, 1989).
- ⁴S. K. Scott, *Chemical Chaos* (Oxford University Press, Oxford, 1991).
- ⁵I. R. Epstein and J. A. Pojman, *An Introduction to Nonlinear Chemical Dynamics* (Oxford University Press, Oxford, 1988).
- ⁶D. Horváth and A. Tóth, *J. Chem. Phys.* **108**, 1447 (1998).
- ⁷A. Tóth, D. Horváth, and A. Siska, *J. Chem. Soc., Faraday Trans.* **93**, 73 (1997).
- ⁸T. Bánsági, Jr., D. Horváth, and A. Tóth, *Phys. Rev. E* **68**, 026303 (2003).
- ⁹T. Bánsági, Jr., D. Horváth, and Á. Tóth, *Chem. Phys. Lett.* **384**, 153 (2004).
- ¹⁰T. Rica, D. Horváth, and A. Tóth, *Chem. Phys. Lett.* **408**, 422 (2005).
- ¹¹A. Zadrazil, I. Z. Kiss, J. D. Hemoncourt, H. Sevcikova, J. H. Merkin, and A. De Wit, *Phys. Rev. E* **71**, 026224 (2005).
- ¹²H. S. Hele-Shaw, *Nature (London)* **58**, 34 (1898).
- ¹³G. García Casado, L. Tofaletti, D. Müller, and A. D'Onofrio, *J. Chem. Phys.* **126**, 114502 (2007).
- ¹⁴T. Bánsági, Jr., D. Horváth, Á. Tóth, J. Yang, S. Kalliadasis, and A. De Wit, *Phys. Rev. E* **68**, 055301 (2003).
- ¹⁵S. Kalliadasis, J. Yang, and A. De Wit, *Phys. Fluids* **16**, 1395 (2004).
- ¹⁶J. W. Wilder, B. F. Edwards, and D. A. Vasquez, *Phys. Rev. A* **45**, 2320 (1992).
- ¹⁷B. F. Edwards, J. W. Wilder, and K. Showalter, *Phys. Rev. A* **43**, 749 (1991).
- ¹⁸D. A. Vasquez, J. W. Wilder, and B. F. Edwards, *J. Chem. Phys.* **98**, 2138 (1993).
- ¹⁹J. W. Wilder, D. A. Vasquez, and B. F. Edwards, *Phys. Rev. E* **47**, 3761 (1993).
- ²⁰D. A. Vasquez, B. F. Edwards, and J. W. Wilder, *Phys. Fluids* **7**, 2513 (1995).
- ²¹A. De Wit, *Phys. Rev. Lett.* **87**, 054502 (2001).
- ²²A. De Wit, *Phys. Fluids* **16**, 163 (2004).
- ²³D. Lima, A. D'Onofrio, and A. De Wit, *J. Chem. Phys.* **124**, 014509 (2006).
- ²⁴M. Leconte, J. Martin, N. Rakotomalala, and D. Salin, *Phys. Rev. Lett.* **90**, 128302 (2003).
- ²⁵J. Huang, D. A. Vasquez, B. F. Edwards, and P. Kolodner, *Phys. Rev. E* **48**, 4378 (1993).
- ²⁶D. A. Vasquez, J. M. Little, J. W. Wilder, and B. F. Edwards, *Phys. Rev. E* **50**, 280 (1994).
- ²⁷D. A. Vasquez, J. W. Wilder, and B. F. Edwards, *J. Chem. Phys.* **104**, 9926 (1996).
- ²⁸J. Huang and B. F. Edwards, *Phys. Rev. E* **54**, 2620 (1996).
- ²⁹D. A. Vasquez and A. De Wit, *J. Chem. Phys.* **121**, 935 (2004).
- ³⁰J. Yang, A. D'Onofrio, S. Kalliadasis, and A. De Wit, *J. Chem. Phys.* **117**, 9395 (2002).
- ³¹J. Masere, D. A. Vasquez, B. F. Edwards, J. W. Wilder, and K. Showalter, *J. Phys. Chem.* **98**, 6505 (1994).